

---

# Microscopic Study of Two Band Superconductivity in Magnesium Diboride Superconductor ( $\text{MgB}_2$ )

Basanta Kumar Sahoo<sup>1,\*</sup>, Biswa Ranjan Mishra<sup>2</sup>, Subhalaxmi Das<sup>3</sup>, Santosh Kumar Barik<sup>1</sup>, Padmaja Patnaik<sup>2</sup>, Ranjan Kumar Bhuyan<sup>1</sup>, Bibekananda Panda<sup>4</sup>

<sup>1</sup>Post Graduate Department of Physics, Government College (Autonomous) Angul, Angul, India

<sup>2</sup>Department of Physics, Centurion University of Technology and Management, Bhubaneswar, India

<sup>3</sup>Department of Physics, Deogarh College, Deogarh, India

<sup>4</sup>Department of Physics, Saraswati Degree Vidya Mandir Neelakantha Nagar, Berhampur, India

## Email address:

basanta@iopb.res.in (B. K. Sahoo)

\*Corresponding author

## To cite this article:

Basanta Kumar Sahoo, Biswa Ranjan Mishra, Subhalaxmi Das, Santosh Kumar Barik, Padmaja Patnaik, Ranjan Kumar Bhuyan, Bibekananda Panda. Microscopic Study of Two Band Superconductivity in Magnesium Diboride Superconductor ( $\text{MgB}_2$ ). *American Journal of Physics and Applications*. Vol. 9, No. 2, 2021, pp. 29-33. doi: 10.11648/j.ajpa.20210902.11

Received: March 15, 2021; Accepted: April 7, 2021; Published: April 26, 2021

---

**Abstract:** We formulate a Model Hamiltonian of two band superconductivity for Magnesium Diboride superconductors ( $\text{MgB}_2$ ). It is a conventional BCS type metallic superconductor which has the highest critical temperature  $T_c=39\text{K}$ . It is assumed that the superconductivity in  $\text{MgB}_2$  arises due to metallic nature of the 2D sheets. From band structure calculations, it is observed that two types of bands i.e.  $\sigma$  and  $\pi$  bands are located at Fermi surface. Here, we consider phonon mediated superconductivity in which  $\sigma$  band is dominant over  $\pi$  band i.e.  $\sigma$  band is more coupled to a superconductor with much higher coupling. We consider a model Hamiltonian with mean field approach and solve this by calculating equations of motion of Green functions for a single particle. We determine the quasi-particle energy from the poles of the Green functions. We derive the single particle correlation functions and determine the two SC order parameters for both  $\sigma$  and  $\pi$  band. Here, the two SC order parameters for the bands are solved self-consistently and numerically. The conduction bandwidth ( $W$ ) is considered as  $W=8t_0$ , where  $t_0$  is the hopping integral. To make all the physical quantities dimensionless, we divide  $2t_0$  in each of the physical quantities. We then calculate the gap ratio  $2\Delta(0)/K_B T_c$  for both the bands. It is seen from our theoretical model that the two bands of  $\text{MgB}_2$  superconductors have two different SC gaps with the same critical temperature. We also observe the variation of dispersion curves of quasi-particles for different temperature parameters for both  $\sigma$  and  $\pi$  band.

**Keywords:** High-  $T_c$  Superconductor, Inter-band Interaction, Mean Field Approximation

---

## 1. Introduction

One of the common, conventional BCS type of superconductor is Magnesium Diboride  $\text{MgB}_2$ . The superconductivity arises due to Cooper pair mechanism through electron – phonon interaction. The mechanism of these type of superconductors is well explained by BCS type of superconductivity [1]. Its critical temperature of 39K is the highest among conventional superconductors and also greater than some of cuprate superconductors where pairing mechanism other than phonons are observed [2, 3].

The structure of  $\text{MgB}_2$  superconductor is hexagonal and the space group is  $p6/mmm$ . Here, Boron atoms are arranged like graphite sheets which are segregated by Magnesium atoms. The Boron atoms in  $\text{MgB}_2$  superconductor form honeycombed layers with magnesium atoms above the centre of hexagons. Specific heat [4, 5] and Tunneling spectroscopy measurements [6], as well as nuclear magnetic resonance (NMR) studies [7] predicts S – wave type superconductivity in  $\text{MgB}_2$  [8, 9]. The presence of isotope effect [11] and pressure dependence of critical temperature [12] predicts the contribution of phono mediated BCS superconductivity. The Fermi surface of  $\text{MgB}_2$  consists of

four sheets, two 3D sheets from the  $\pi$  bonding with antibonding ( $B - 2P_z$ ) and other two nearly cylindrical sheets from 2D  $\sigma$  bonding ( $B - 2P_{x,y}$ ) [13, 14]. Experiments such as point-contact spectroscopy [15], specific heat measurement [4, 5], scanning tunneling microscopy [16] and Raman spectroscopy [17], critical current measurement [18] clearly explain the existence of two distinct superconducting gaps with small gaps  $\Delta_S(0)=2.8 \pm 0.05$  MeV and large gap  $\Delta_L(0)=7.1 \pm 0.1$  MeV [19]. Both gaps close near the bulk transition temperature  $T_C=39$ K. This case has been predicted theoretically by Liu *et al* [13]. With  $T_C = 39$ K and two distinct superconducting gaps, MgB<sub>2</sub> serves as an important test case for Density Functional Theory (DFT) for superconductors.

There is substantial evidence from the band structure calculation that strong covalent bonds are formed between Borons and after the ionization of Mg, two of its electrons is transferred to the conduction band which is formed by Borons [20]. So, it is believed that superconductivity in MgB<sub>2</sub> is primarily contributed from 2D metallic sheets of Boron. It is concluded that MgB<sub>2</sub> is a typical type II superconductor with Ginsburg-Landau parameter  $K \approx 23$  [21]. It is observed that there is a substantial reduction in isotope effect from the BCS predicted value of 0.5. The critical temperature ( $T_C$ ) in MgB<sub>2</sub> depends upon boron substitution whereas there is no appreciable change due to Mg isotopic substitution. So, the isotopic coefficient due to boron ( $\alpha_B$ ) has a significant role while the contribution due to isotopic coefficient of Magnesium ( $\alpha_{Mg}$ ) is very small. It is reported

$$H = \sum_{k,\sigma} (\epsilon_k^a - \mu) a_{k,\sigma}^\dagger a_{k,\sigma} + \sum_{k,\sigma} (\epsilon_k^b - \mu) b_{k,\sigma}^\dagger b_{k,\sigma} - \sum_{k,k'} V_{aa}(k, k') a_{k\uparrow}^\dagger a_{-k\downarrow}^\dagger a_{k'\downarrow} a_{k'\uparrow} - \sum_{k,k'} V_{bb}(k, k') b_{k\uparrow}^\dagger b_{-k\downarrow}^\dagger b_{k'\downarrow} b_{k'\uparrow} - \sum_{k,k'} V_{ab}(k, k') a_{k\uparrow}^\dagger a_{-k\downarrow}^\dagger b_{k'\downarrow} b_{k'\uparrow} + cc \quad (1)$$

Equation (1) represents the total Hamiltonian of our system where both the first and second term represents the Hamiltonian due to hopping of quasi-particles of  $\pi$  and  $\sigma$  band. Here,  $a_{k,\sigma}^\dagger(a_{k,\sigma})$  represents the creation and annihilation operators for  $\sigma$  band and  $b_{k,\sigma}^\dagger(b_{k,\sigma})$  represents the same for  $\pi$  band for conduction electrons. One particle kinetic energy for  $\sigma$  and  $\pi$  band are  $\epsilon_k^a$  and  $\epsilon_k^b$  with  $\mu$  is the chemical potential.

It was assumed that, due to boson exchange, an S – wave

$$H = \epsilon_\sigma \sum_k (a_{k\uparrow}^\dagger a_{k\uparrow} + a_{k\downarrow}^\dagger a_{k\downarrow}) + \epsilon_\pi \sum_k (b_{k\uparrow}^\dagger b_{k\uparrow} + b_{k\downarrow}^\dagger b_{k\downarrow}) - \Delta_\sigma \sum_k (a_{k\uparrow}^\dagger a_{-k\downarrow}^\dagger + a_{-k\downarrow} a_{k\uparrow}) - \Delta_\pi \sum_k (b_{k\uparrow}^\dagger b_{-k\downarrow}^\dagger + b_{-k\downarrow} b_{k\uparrow}) + V_1 \sum_k (a_{k\uparrow}^\dagger a_{-k\downarrow}^\dagger + a_{-k\downarrow} a_{k\uparrow}) + V_2 \sum_k (b_{k\uparrow}^\dagger b_{-k\downarrow}^\dagger + b_{-k\downarrow} b_{k\uparrow}) \quad (2)$$

Where,

$$\begin{aligned} \epsilon_\sigma &= \epsilon_k^a - \mu, \epsilon_\pi = \epsilon_k^b - \mu \\ \Delta_\sigma &= V_{aa} \langle a_{k\uparrow}^\dagger a_{-k\downarrow}^\dagger \rangle = V_{aa} \langle a_{-k\downarrow} a_{k\uparrow} \rangle \\ \Delta_\pi &= V_{bb} \langle b_{k\uparrow}^\dagger b_{-k\downarrow}^\dagger \rangle = V_{bb} \langle b_{-k\downarrow} b_{k\uparrow} \rangle \\ V_1 &= V_{ab} \langle a_{k\uparrow}^\dagger a_{-k\downarrow}^\dagger \rangle = V_{ab} \langle a_{-k\downarrow} a_{k\uparrow} \rangle \\ V_2 &= V_{ab} \langle b_{k\uparrow}^\dagger b_{-k\downarrow}^\dagger \rangle = V_{ab} \langle b_{-k\downarrow} b_{k\uparrow} \rangle \end{aligned}$$

For simplicity of calculation, we consider the inter-band

by Budko *et al* about the measured value of  $\alpha_B=0.26$  [10]. Hinks *et al* predicted an  $\alpha_B$  of 0.30 and  $\alpha_{Mg}$  of 0.02 [11]. For MgB<sub>2</sub>, the total isotope coefficient is 0.32 with a high Debye temperature of  $\theta_D=750$  K. Optical measurement [22] and the specific heat measurement [5] roughly estimates the value of  $\frac{2\Delta(0)}{k_B T_C} \approx 4.2$  which deviates from the BCS value of 3.53 [23]. MgB<sub>2</sub> is the first material where the multi gap effects are dominant and its transition temperature has been supported with electron-phonon interaction mechanism for the superconductivity. The nature of multiple gaps had been discussed theoretically [24, 25]. Here, We formulate a two-band Hamiltonian model to study the multi gaps in MgB<sub>2</sub> and we use Zubarev type Green function technique [26]. In the introduction, we have reviewed the experimental observations of MgB<sub>2</sub> superconductors. We explain the Hamiltonian model where we consider SC pairing mechanism of BCS type in Section – 2. We will define suitable Green functions and find the expressions of SC order parameters for both  $\sigma$  and  $\pi$  bands. The results of the numerical calculation are discussed in Section-3. Finally, the conclusion is given in Section-4.

## 2. Model Hamiltonian and Calculation of SC Order Parameter

The two band BCS Hamiltonian for our system is

type BCS pairing interaction exists in  $\pi$  and  $\sigma$  band. The inter band superconductivity of  $\sigma$  and  $\pi$  band are represented by the third and fourth term of equation (1) respectively. The inter-band pairing interaction for  $\sigma$  and  $\pi$  are represented by  $V_{aa}$  and  $V_{bb}$  respectively. The fifth term represents the Hamiltonian involving inter-band pairing between  $\sigma$  and  $\pi$  electrons. The inter-band pairing interaction is  $V_{ab}$ .

The Hamiltonian of the equation (1) in the mean-field form is

pairing exchange interaction strength  $V_1 \approx V_2 = V$ . We calculate one electron Green's function given in equation (2) in the super conducting state of MgB<sub>2</sub> system. The double time electron Green function is calculated by equation of method [27-29]. The four number of Green's functions  $A_1(k, \omega)$ ,  $A_2(k, \omega)$ ,  $B_1(k, \omega)$  and  $B_2(k, \omega)$  are involved in the calculation.

$$A_1(k, \omega) = \langle \langle a_{k\uparrow}; a_{k\uparrow}^\dagger \rangle \rangle_\omega$$

$$A_2(k, \omega) = \langle \langle a_{-k\downarrow}^\dagger; a_{k\uparrow}^\dagger \rangle \rangle_\omega$$

$$B_1(k, \omega) = \langle \langle b_{k\uparrow}; b_{k\uparrow}^\dagger \rangle \rangle_\omega$$

$$B_2(k, \omega) = \langle\langle b_{-k\downarrow}^\dagger; b_{k\uparrow}^\dagger \rangle\rangle_\omega$$

The equations of motion of the Green function  $A_1, A_2, B_1, B_2$  are

$$A_1 = \frac{1}{2\pi} \left[ \frac{\omega + \epsilon_1(k)}{\omega^2 - \epsilon_2(k)^2 + (\Delta_\sigma + V)^2} \right] \quad (3)$$

$$A_2 = \frac{1}{2\pi} \left[ \frac{\omega + \epsilon_2(k)}{\omega^2 - \epsilon_2(k)^2 + (\Delta_\pi + V)^2} \right] \quad (4)$$

$$B_1 = \frac{1}{2\pi} \left[ \frac{-(\Delta_1 + V)}{\omega^2 - \epsilon_1(k)^2 + (\Delta_\sigma + V)^2} \right] \quad (5)$$

$$B_2 = \frac{1}{2\pi} \left[ \frac{-(\Delta_2 + V)}{\omega^2 - \epsilon_2(k)^2 + (\Delta_\pi + V)^2} \right] \quad (6)$$

The Green functions required for calculating SC order parameter is  $A_2$  and  $B_2$ . The poles of the Green functions are

$$W_{1,2} = \pm \sqrt{(\Delta_\sigma + V)^2 + \epsilon_1^2(k)}$$

$$W_{3,4} = \pm \sqrt{(\Delta_\pi + V)^2 + \epsilon_2^2(k)}$$

The SC gaps parameters for  $\sigma$  and  $\pi$  bands are calculated from the Green's functions  $A_2(k)$  and  $B_2(k)$  respectively. Here,  $W_{1,2}$  and  $W_{3,4}$  are quasiparticle energies which are calculated from the poles of the Green Functions. The expressions for  $\Delta_\sigma$  and  $\Delta_\pi$  are

$$\Delta_{\sigma,k} = -\sum_k \tilde{V}_{\sigma,k} (\langle\langle a_{k\uparrow}^\dagger a_{-k\downarrow}^\dagger \rangle\rangle)$$

$$\Delta_{\pi,k} = -\sum_k \tilde{V}_{\pi,k} (\langle\langle b_{k\uparrow}^\dagger b_{-k\downarrow}^\dagger \rangle\rangle)$$

For simplification, we drop  $k$  and  $\omega$  dependence in the Green functions. Each of the bands is a function of SC gap parameter and inter band pairing exchange interaction. Here, we use BCS type of Cooper pairing due to phonons between conduction electrons in each band. The attractive interaction is valid with energy  $|\epsilon_1 - \epsilon_2| < \omega_D$ . Here, the attractive interactions between two carriers are  $\epsilon_1$  and  $\epsilon_2$  to form the Cooper pairs within the range of Debye frequency ( $\omega_D$ ). We have adopted here the interaction potential  $\tilde{V}_k$  in the ordinary isotropic weak coupling limit. Here  $\tilde{V}_k = -V_0$ , if  $|\epsilon_1 - \epsilon_2| < \omega_D$ ,  $\tilde{V}_k = 0$ , otherwise. In this approximation, we consider the SC gap is independent of  $k$ .

$$\Delta_\sigma(T) = V_0(\sigma) N_\sigma(0) \int_{-\omega_{D1}}^{\omega_{D1}} d[\epsilon_0(k)] \times \left( \frac{\Delta_\sigma + V}{\omega_1 - \omega_2} \right) \left[ \frac{1}{1 + \exp(\beta\omega_1)} - \frac{1}{1 + \exp(\beta\omega_2)} \right] \quad (7)$$

$$\Delta_\pi(T) = V_0(\pi) N_\pi(0) \int_{-\omega_{D2}}^{\omega_{D2}} d[\epsilon_0(k)] \times \left( \frac{\Delta_\pi + V}{\omega_1 - \omega_2} \right) \left[ \frac{1}{1 + \exp(\beta\omega_3)} - \frac{1}{1 + \exp(\beta\omega_4)} \right] \quad (8)$$

Different physical quantities used in the calculation are superconducting gap parameters ( $\Delta_{\sigma,\pi}(T)$ ), the inter pair exchange interaction strength ( $V$ ), the density of states ( $N_{\sigma,\pi}(0)$ ), the Debye frequencies  $\omega_D$  and temperature ( $T$ ). We divide  $2t_0$  in each of the physical quantities involved in the calculation, where  $W = 8t_0$  is the width of the conduction band. The dimensionless parameters are SC order parameter for  $\sigma$  band  $\frac{\Delta_\sigma(T)}{2t_0} = Z_\sigma$ , SC order parameter for  $\pi$  band  $\frac{\Delta_\pi(T)}{2t_0} = Z_\pi$ , Debye frequency for  $\sigma$  band  $\frac{\omega_{D1}}{2t_0} = \tilde{\omega}_{d1}$ , Debye frequency for  $\pi$  band  $\frac{\omega_{D2}}{2t_0} = \tilde{\omega}_{d2}$ , reduced temperature  $\frac{K_B T}{2t_0} = \theta$ , Inter pair exchange interaction constant  $\frac{V}{2t_0} = V$ , SC coupling constant for  $\sigma$  band  $g_1 = N_\sigma(0)V_0(\sigma)$  3. and SC coupling constant for  $\pi$  band  $g_2 = N_\pi(0)V_0(\pi)$ .

### 3. Result and Discussion

We have self-consistently and numerically solved the SC gaps  $Z_\sigma(T)$  and  $Z_\pi(T)$ . All the physical parameters are in dimensionless form. The dimensionless parameters are SC coupling constant ( $g_1$ ) for  $\sigma$  band, SC coupling constant ( $g_2$ ) for  $\pi$  band, SC gap parameter  $Z_\sigma$  for  $\sigma$  band, SC gap parameter  $Z_\pi$  for  $\pi$  band, inter pair exchange interaction constant ( $V$ ), Debye frequency ( $\omega_D$ ) and temperature parameter ( $\theta$ ). The Fermi level  $\epsilon_F$  is in the half position of the conduction band i.e.  $\epsilon_F = 0$ . We consider the conduction bandwidth  $W_b$  where  $W_b = 8t_0 \approx 1eV$ .

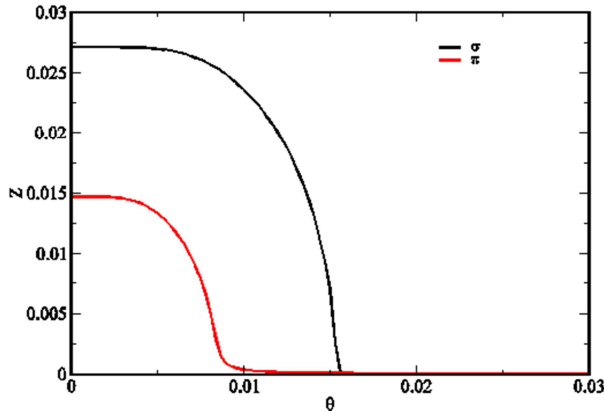
Figure 1 depicts the temperature dependence SC-gap for both  $\sigma$  and  $\pi$  bands of Magnesium diboride superconductor.

The critical temperature parameter for both the bands is ( $\theta_c$ )=0.1565 equivalent to 39.1K. The SC-gap value for  $\sigma$ -band is  $0.0271 \approx 6.78$  MeV. The observed gap ratio  $\frac{2\Delta(0)}{K_B T_c} = \frac{2Z}{K_B \theta_c} = 3.47$  which is slightly less than the universal BCS value of 3.52. The SC-gap value for  $\pi$  band is  $0.0145 \sim 3.62$  MeV and the gap ratio  $\frac{2\Delta(0)}{K_B T_c} = \frac{2Z}{K_B \theta_c} = 1.85$ . Earlier, Liu *et al* [30] predicted that the critical temperature for both the bands is 39K where our theoretical result gives 39.1 K. The value of SC gap in  $\sigma$  band is in between 6.4 MeV to 7.2 MeV and for  $\pi$  band, it is between 1.2 to 3.7 MeV as reported earlier by Choi *et al* theoretically [31]. The same two SC gaps as reported experimentally range from 5.5 MeV to 8 MeV for  $\sigma$  band and 1.5 MeV to 3.5 MeV for  $\pi$  band [32-34]. For the observed theoretical result, we have taken the SC coupling constant of  $\sigma$  band ( $g_1 = 0.33$ ) and the SC coupling constant of  $\pi$  band ( $g_2 = 0.285$ ). Here we have considered the phonon mediated superconductivity which shows that  $\sigma$  band is dominant in  $MgB_2$  superconductors with a stronger coupling and  $\pi$  band is less coupled to the superconductors with a much weaker coupling which agrees well with the experiment [35 - 37]. We also observed two-bands i.e.  $\pi$  band and  $\sigma$  band having two different SC-energy band gaps with the same critical temperature of 39.1 K from our theoretical model calculation and the gap ratio is approximately the same as experimentally and theoretically observed value [30-33, 38].

Figure 2 depicts the quasi-particle energy plots ( $W_\sigma$  and  $W_\pi$ ) vs.  $x_0$  ( $x_0 = \frac{\epsilon_0(K)}{2t_0}$ ) for temperature parameter ( $\theta=0K$ ). Here the quasi particle energy of  $\sigma$  band and  $\pi$  band are

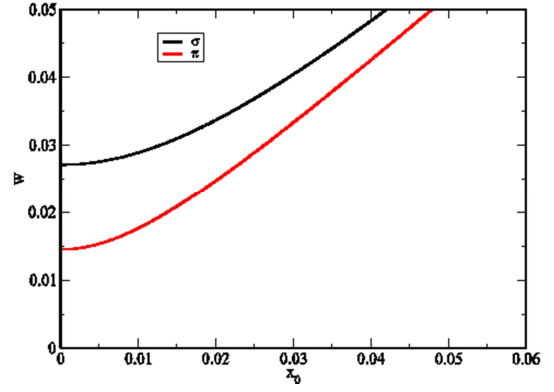
$W_1=6.78$  MeV and  $W_3=3.625$  MeV respectively. To study the nature of the plot, we only consider the positive part of quasiparticle energy. These bands show a strong dependence on energy  $\epsilon_0(K)$ . The separation between gaps decreases when the energy  $\epsilon_1(K)$  increases and shows the dispersion of the  $\sigma$  and  $\pi$  band which also differ considerably. For  $\sigma$  band, the most prominent dispersion was observed and these bands are nearly flat bands. In our model, the plot shows the  $\sigma$  band has more prominent dispersion than  $\pi$  band. It is clear from figure 2 that the trend of  $\sigma$  band shows slightly flat than  $\pi$  band at low temperature which agrees well with the experiment [39, 40]. The dispersed flat band indicates the system as a strongly correlated one. The dispersion of quasi-particles mentioned here agrees well with the band dispersion of quasi-particles reported earlier [41-43].

Figure 3 depicts the variation of the quasiparticle energy band of  $W_\sigma$  vs.  $x_0$  for different temperature Parameters. At  $\theta=0K$ , the band shows flat nature. As temperature increases ( $\theta=0K$  to  $\theta=37.5K$ ) the dispersion plots shows the same trend but for the temperature  $\theta=0K$ , the plot is more dispersed than the dispersion plot of other temperature. With the increase in temperature parameter from  $\theta=0K$  to  $\theta=37.5K$ , the quasiparticle energy decreases from 6.78K to 1.73K. However, it is found that the quasiparticle energy depends upon the magnitude of the SC gap at the respective temperature parameters.



**Figure 1.** Two SC gaps ( $z$ ) for  $\sigma$  and  $\pi$  band vs. temperature parameter ( $\theta$ ) solved self-consistently. The value of different dimensionless parameters are inter-band pairing constant ( $V$ )  $\approx 0.00002$ , SC coupling constant of  $\sigma$  band ( $g_1=0.33$ ), SC coupling constant of  $\pi$  band ( $g_2=0.285$ ), Debye frequency for  $\sigma$  band ( $\omega_{d2}$ ) $\approx 0.281 \approx 787.7$  K, Debye frequency for  $\pi$  band ( $\omega_{d1}$ ) $\approx 0.26 \approx 650$  K.

Figure 4 depicts the quasiparticle energy of  $\pi$  band for the same four temperature parameters. The value decreases from 0.625 MeV to 0.0275 MeV as we move from temperature parameters  $\theta=0K$  to  $\theta=37.5K$ . The energy  $W_\pi$  at  $\theta=0K$  disperses more than the dispersion curve of the other two temperatures. The separation of dispersion is more prominent at  $x_0$  tends to zero and the separation decreases towards higher values of  $\theta$ .



**Figure 2.** Quasi-particle energy ( $W_\sigma$  and  $W_\pi$ ) vs.  $x_0$  ( $x_0 = \frac{\epsilon_0(K)}{2t_0}$ ) for temperature parameter ( $\theta = 0K$ ).

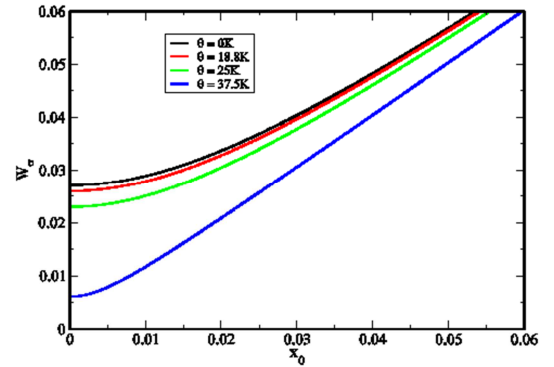


**Figure 3.** Plot of quasiparticle energy bands of  $W_\sigma$  vs.  $x_0$  for different temperature Parameters for  $\sigma$  band.

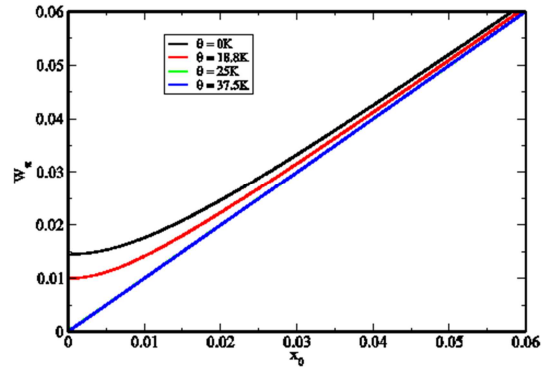


**Figure 4.** Plot of quasiparticle energy bands of  $W_\pi$  vs.  $x_0$  for same four temperature Parameters for  $\pi$  band.

## 4. Conclusion

We report two SC-gaps in MgB<sub>2</sub> superconductor by taking mean-field levels calculations of Green functions technique. The equation of motions, quasi-particle energy for  $\sigma$  and  $\pi$  band are derived. We have calculated the correlation functions. The two SC-order parameters for the  $\sigma$  band and  $\pi$  band are derived. The SC-energy gap and critical temperature for the two bands of MgB<sub>2</sub> superconductor are calculated. It is found that the critical temperature for both bands remains the same with two different energy gap which agrees well with the experiment. The nature of dispersion curves of quasi-particle energy is also studied. This model can be improved by adding an external magnetic field in both bands

to study the SC-gaps in the two-band model.

## Acknowledgements

The authors Basanta Kumar Sahoo, Bibekananda Panda and Subhalaxmi Das are grateful to the Director, Institute of Physics, Bhubaneswar, Odisha, India for providing facilities in the vacation.

## References

- [1] J. Bardeen, L. N. Cooper, J. R. Schrieffer, *Phys. Rev* 106 162 (1957).
- [2] H. B. Schuttler, C. H. Pao, *Phys. Rev. Lett.* 75 4504 (1995).
- [3] P. W. Anderson, *Theory of Superconductivity in the High-Tc Cuprates*, Princeton NJ (1997).
- [4] F. Bouquet, R. A. Fisher, N. E. Philips, Y. Wang, D. G. Hinks, J. D. Jorgenser, A. Junod, *Europhys Lett.* 56 856 (2001).
- [5] Y. Wang, T. Plackonwski, A. Junod, *Physica C* 355 179 (2001).
- [6] A. Sharoni, I. Felner, O. Millo, *Phys. Rev. B* 63 220508 (2001).
- [7] H. Kotegawa, K. Ishida, Y. Kitaoka, T. Muranaka, J. Akimitsu, *Phys. Rev. Lett.* 87 127001 (2001).
- [8] S. Hass, K. Maki *Phys. Rev. B* 65 020502 (R) (2001).
- [9] Y. Chen, K. Mani *Current Applied Physics* 1, 4-5, 33 (2001).
- [10] S. L. Budko, G. Lapertot, C. Petrovic, C. E. Cunningham, N. Anderson, P. C. Canfield, *Phys. Rev. Lett* 86 1877 (2001).
- [11] D. G. Hinks, H. Claus, J. D. Jorgensen, *Nature* 411 458 (2001).
- [12] G. Karapetrov, M. Iavarone, W. K. Kwok, G. W. Crabtree, D. G. Hinks, *Cond-mat/0102312*.
- [13] A. Y. Liu, I. I. Mazin, J. Kortus, *Phys. Rev. Lett* 87 087005 (2001).
- [14] H. J. Choi, M. L. Cohen, S. G. Louie, *Physica C* 345 66 (2003).
- [15] H. Schmidt, J. F. Zasadzinski, K. E. Gray, D. G. Hinks, *Cond-mat/0112144* (2002).
- [16] F. Giubileo, D. Roditchev, W. Sacks, R. Lamy, D. X. Thanh, T. Keli, S. Miraglia, D. Fruchart, J. Marcus, Ph. Monod, *Phys. Rev. Lett.* 87 177008 (2001).
- [17] X. K. Chen, M. J. Korstantinovic, J. C. Irwin, D. D. Lawrie, J. P. Franck, *Cond-mat/0104005*.
- [18] Glowacki, Bartek A.; Wozniak, Marcin *Acta Physica Polonica A*; 5 (138), pp. 695-704 (2020).
- [19] R. E. Lagos, G. G. Cabrera, *Braz. J. Phys.* 33 14 (2003).
- [20] J. Kortus, I. I. Mazin, K. D. Belashchenko, V. P. Antropov, L. L. Boyer, *Phys. Rev. Lett.* 86 4656 (2001).
- [21] T. S. Kayed, *Crystal Research and Technology* 39, 50 (2004).
- [22] R. da Silva, J. H. S. Torres, Y. Kopelevich, *Cond-mat/0105329* (2001).
- [23] K. Vinod, N. Verghese, U. Symaprasad, *Superconductor Science and technology* 20 (10) R31 (2007).
- [24] H. Suhl, B. T. Matthis, R. Walker, *Phys. Rev. Lett.* 3, 552 (1959).
- [25] J. Kondo, *Pro. Theo Phys* 8 (1959) 25.
- [26] D. N. Zubarev, *Sov. Physics. Usp.* 95 (1960) 71.
- [27] B. K Sahoo, B. N. Panda, *Physica C* 470, 547 (2010).
- [28] B. K Sahoo, B. N. Panda, F. T. Dias, *Int. journal of adv. Technology in eng. and science* 11 445-450 (2014).
- [29] G. C. Rout, S. Das, *Physica C* 339, 17-26 (2000).
- [30] A. Y. Liu, I. I. Mazin, J. Kortus, *Cond. mat* (2001) 0103570.
- [31] H. J. Choi, D. Roundy, H. Sun, M. L. Cohen, S. G. Louie, *Nature.* 418 (2002) 6899, 758-760.
- [32] K. X. Chen, M. J. Konstantinovi, J. C. Irin, D. D. Lowrie J. P. Frank *Phys. Rev. Lett.* 87, 157002-1-157002-4 (2001).
- [33] S. Tsuda, T. Yokoya, T. Kiss, Y. Takano, K. Togano, H. Kito, H. Ihara, S. Shin, *Phys. Rev. Lett.* 87, 157002-1-157002-4 (2001).
- [34] C. Buzea, T. Yamashita *Super Cond. Sci. Technol.* 14, R115-R146 (2001).
- [35] H. Schmidt, J. F. Zasadzinski, K. E. Gray, D. G. Hinks, *Physics Rev. B* 63 (220504) R (2001).
- [36] A. Sharoni, I. Felner, O. Millo *Physics Rev. B* 63 (220508) R (2001) G. Karapetrov, L. Iavarone, W. K. Kwok, G W Crabtree, D. G. Hinks *Phys. Rev. Lett.* 86, 4374 (2001).
- [37] G. Karapetrov, L. Iavarone, W. K. Kwok, G W Crabtree, D. G. Hinks *Phys. Rev. Lett.* 86, 4374 (2001).
- [38] Hyunsoo Kim, Kyuil Cho, Makariy A. Tanatar, V. Toufour, S. K. Kim, S. L. Budco, V. G. Kogan, R. Projorov, *Symmetry*, 11 (8) 1012 (2019).
- [39] II Mazin and Antropov *Physics C* 385 (2003) 4.
- [40] N. I Medvedea, A L Ivanovskii, J E Medvedeve and A J Freeman *Phys Rev. B* 64 (2001) 020502.
- [41] P. Fulde, *Journal of low temperature physics* 95 (1994).
- [42] B. K Sahoo, B. N. Panda: *PRAMAN Journal of Physics* 77 (2011).
- [43] Ian D. R. Mackinnon, Peter C. TalbotJose, A. Alarco *Computational Materials Science* 130 (2017) 191-20.